

Journal of Materials Chemistry C

Accepted Manuscript



This article can be cited before page numbers have been issued, to do this please use: R. Singh, H. Wu, A. K. Dwivedi, A. Singh, C. Lin, P. Raghunath, M. C. Lin, T.-K. Wu, K. Wei and H. Lin, *J. Mater. Chem. C*, 2017, DOI: 10.1039/C7TC03071A.



This is an Accepted Manuscript, which has been through the Royal Society of Chemistry peer review process and has been accepted for publication.

Accepted Manuscripts are published online shortly after acceptance, before technical editing, formatting and proof reading. Using this free service, authors can make their results available to the community, in citable form, before we publish the edited article. We will replace this Accepted Manuscript with the edited and formatted Advance Article as soon as it is available.

You can find more information about Accepted Manuscripts in the [author guidelines](#).

Please note that technical editing may introduce minor changes to the text and/or graphics, which may alter content. The journal's standard [Terms & Conditions](#) and the ethical guidelines, outlined in our [author and reviewer resource centre](#), still apply. In no event shall the Royal Society of Chemistry be held responsible for any errors or omissions in this Accepted Manuscript or any consequences arising from the use of any information it contains.



Journal of Materials Chemistry C

ARTICLE

Monomeric and aggregation emissions of tetraphenylethene in a photo-switchable polymer controlled by cyclization of diarylethene and solvent conditions

Received 00th January 20xx,
Accepted 00th January 20xx

DOI: 10.1039/x0xx00000x

www.rsc.org/

Ravinder Singh,^a Hsin-Yen Wu,^a Atul Kumar Dwivedi,^a Ashutosh Singh,^a Chien-Min Lin,^a Putikam Raghunath,^b Ming-Chang Lin,^b Tung-Kung Wu,^c Kung-Hwa Wei^a and Hong-Cheu Lin*^a

A novel photo-switchable polymer **P-PHT** containing diarylethene (DAE), tetraphenylethene (TPE) moieties and a triazole linker in the repeating unit was synthesized to study the aggregation-induced emission (AIE) behaviour of TPE in both open and close forms of DAE in **P-PHT** with high water contents. The photo-switching phenomena of DAE (from open to close form under UV-irradiation) in **P-PHT** were prominent in organic solvent (THF), high water contents (at 90% H₂O) and acidic conditions. Upon UV-irradiation of **P-PHT** at 90% water content, the AIE of TPE was completely quenched via energy transfer event from TPE to cyclized DAE. Interestingly, the rare monomeric emission of TPE was first discovered by the photo-cyclization of DAE in **P-PHT** compared with the AIE behaviour of TPE in the open form of DAE in **P-PHT** with AIE favourable conditions of high water contents (90% H₂O) and acidic conditions.

1. Introduction

Among various photo-switchable units, many researchers have been attracted to diarylethenes (DAEs) due to their excellent characteristics,¹ such as thermal stability, fatigue resistance, high sensitivity,² and response in various states.³⁻⁶ The ease of introducing organic functionalities to DAE units resulted in a variety of fluorescent DAE derivatives by means of cyclization for the applications of optical memory,^{7,8} intra-molecular energy transfer,⁹⁻¹⁸ and electron transfer.¹⁹⁻²¹ The photo-switching activities of DAEs could be facilitated by several factors, including structural conformations of open-ring isomers, electron donor/acceptor substituents, conjugation lengths of hetero-aryl groups and other external stimuli (e.g., pH, cations, anions and biomolecules).²²⁻³³ Moreover, due to better film qualities of polymers, photochromic DAE-based polymers are preferred than small molecules for their practical applications in the areas of optoelectronics, photonics and linear and nonlinear optics.^{34,35}

Nowadays, the aggregation-induced emission (AIE) phenomenon of tetraphenylethene (TPE) fluorophore has attracted much attention since it has been first introduced by

Tang and co-workers in 2001.^{36,37} AIE is an excellent behaviour of TPE that is caused by the restriction of intra-molecular rotations (RIR) of connected periphery phenyl rings in aggregates. The TPE unit also acts as an energy donor moiety with the combination of some other fluorophores reported in many literatures.^{38,39} Furthermore, with the fruitful advantages of AIE effects for practical applications, a large variety of AIE-based probes in the area of chemo- and bio-sensors,^{40,41} biomedical imaging processes,⁴² OLED devices,⁴³ optical waveguides,⁴⁴ and liquid crystal displays with efficient solid-state emissions have been widely explored and developed.^{45,46} Besides, many AIE-based fluorescent probes for pH detections have been successfully created⁴⁷ by taking accountable principles of AIE-based pH sensing processes that are dis-aggregations and aggregations of AIEgens in different pH environments.

There are very few reports on photo-switching activities of DAEs coupled with other fluorophores (or chromophores),⁴⁸⁻⁵⁰ i.e., tetraphenylethenes (TPEs), so it would be remarkable to incorporate novel properties of energy/electron transfer from TPEs to DAEs into a main-chain AIE-active polymer. Moreover, TPE-based polymeric materials possess numerous advantages, such as ease of processability and functionalization, structural diversity and good thermal stability, which supply them with great potentials in practical applications in contrast to AIE-active small molecules.⁵¹⁻⁵⁶ Therefore, constructing novel polymers with the combination of DAE and TPE might be quite interesting towards disclosing important associated properties. Additionally, monomeric emissions of TPEs are rare and till date only two reports presented such emissions in mono-chromophoric systems.^{57,58}

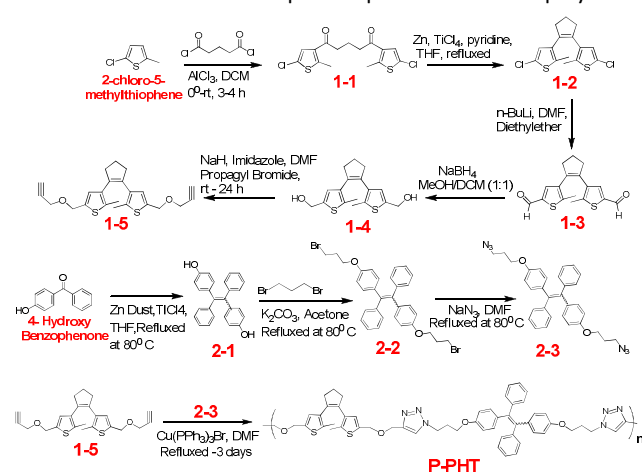
^a Department of Materials Science & Engineering, National Chiao Tung University, Hsinchu 300, Taiwan *linhc@mail.nctu.edu.tw

^b Center for Interdisciplinary Molecular Science, Department of Applied Chemistry, National Chiao Tung University Hsinchu 300, Taiwan

^c Department of Biological Science & Technology, National Chiao Tung University, Hsinchu 300, Taiwan

Electronic Supplementary Information (ESI) available: [details of any supplementary information available should be included here]. See DOI: 10.1039/x0xx00000x

As described in the literature, because the photo-switching DAE moiety attached to the fluorophore directly (or through a short linker) would induce opposite energy transfer rather than cyclization,⁵⁹⁻⁶¹ no photochromism could be observed. This problem can be overwhelmed by introducing a flexible spacer between the DAE moiety and fluorophore, so we insert the flexible spacer in our molecular design to explore the energy transfer event. Herein, we report a novel polymer **P-PHT** consisting of DAE and TPE units with a protonable triazole linker via Cu(I) catalyzed click reaction and its synthetic route is shown in Scheme 1, where the cyclization of DAE in both organic solvent (THF) and 90% water were significant as monitored the energy transfer event from TPE to DAE. The Cu(I)-catalyzed azide-alkyne cycloaddition is popularly known as the click reaction.⁶² Nowadays, click chemistry has found widespread applications in various research areas, such as triazole-based polymers,⁶³ dendrimers⁶⁴ and post-functionalized polymers.⁶⁵ Since the click reaction adores the benefits of mild reaction conditions, high efficiencies and regioselectivities along with simple purification procedures, it has become a powerful synthetic tool with applicability in different research fields.⁶⁶ In this study, we adopted such click reaction to prepare our photo-switchable polymer. The photo-switchable phenomena of a designed DAE derivative connected with tetraphenylethene (TPE) via a spacer are explored in various aqueous conditions and/or different pH environments (to incorporate protonable moieties). During the photo-switching of DAE (from open to close form under UV-irradiation), the generation of monomeric emission with simultaneous quench of aggregation-induced emission (AIE) of TPE occurred in high water content (90% H₂O), which might be considered as the first example of a photo-switchable polymer.



Scheme 1. Synthetic route of **P-PHT**.

2. Experimental

Materials and characterization

All commercial available starting materials 2-chloro-5-methylthiophene, 4-hydroxy benzophenone and glutaryl

chloride with analytical purity were used and dry solvents were obtained by distillation over appropriate drying agents. By following standard procedures, all moisture sensitive reactions were carried out under N₂ gas atmosphere to avoid moisture and the product formations were monitored via visualized the TLC plates under ultra-violet light (256 nm). The merck silica gel 60 (230-400 mesh) was used for column chromatography to purified the desired products and the reported yields are isolated yields. By using 1 cm quartz cuvette the corresponding UV-Vis spectra and fluorescence measurements were conducted in a Jasco UV-600 spectrophotometer and HITACHI 4000 series spectrophotometer, respectively. All emission and excitation spectra were corrected for the detector response and the lamp output. The molecular weight of the polymer (**P-PHT**) was measured by gel permeation chromatography (GPC) using Waters 1515 (isocratic HPLC pump) and 2414 (reflective index detector) instruments and eluting with tetrahydrofuran (THF). The UV-irradiation was carried out using a 500 W Xenon arc lamp (Solar Electro-Optics Co., LTD) with an intensity of 1.17 mW/cm² as the light source. Mass spectra (HRMS) were obtained on the respective mass spectrometer. In order to investigate the surface morphologies and particle size distributions of **P-PHT**, thus the corresponding experiments were performed by using a thermal field emission scanning electron microscope (SEM) (JEOL JSM-6500 F). SEM samples of **P-PHT** were prepared by drop-casting onto Si wafers followed by vacuum drying under room temperature. Furthermore, the dynamic light scattering (DLS) analyses were studied by using a Malvern instruments-Zetasizer nano ZS90.

NMR spectra were recorded on Bruker DRX-300 Avance series (¹H: 300 MHz; ¹³C: 300 MHz) at a constant temperature of 298 K and chemical shifts were reported in parts per million (ppm) from low to high field, referenced to residual solvents (CDCl₃ δ = 7.26 ppm and δ = 77.23 ppm; DMSO-*d*₆ δ = 2.49 ppm and δ = 39.56 ppm, respectively) and tetramethylsilane SiMe₄ (TMS) was used as internal reference for the ¹H and ¹³C-NMR analyses. The coupling constant (*J*) were reported in hertz (Hz). Standard abbreviations indicating multiplicity were used as follows: s = singlet, d = doublet, dd = double doublet, t = triplet, m = multiplet, br = broad.

Synthetic procedure of intermediates

Synthesis of 1,5-bis(5-chloro-2-methylthiophen-3-yl)pentane-1,5-dione (1-1) and 1,2-bis(5-chloro-2-methylthiophen-3-yl)cyclopent-1-ene (1-2). Synthesis of intermediates **1-1** and **1-2** were performed by following the reported synthetic procedure in the literature.^{61,62}

ESI-HRMS of **1-1**= Chemical Formula: C₁₅H₁₅Cl₂O₂S₂, Measured (M/Z): 360.9885. Calculated (M/Z) = 360.9887 [M+H]⁺.

Synthesis of intermediate 2-3. Intermediate **2-3** was successfully synthesized in our previous report and carried forward for this project.³⁷

¹H-NMR (300 MHz, DMSO-*d*₆) δ (ppm): 7.07-7.15 (6H, m), 6.98 (4H, m), 6.88-6.93 (4H, m), 6.67-6.70 (4H, m), 3.95 (4H, t, *J* = 6.0 Hz, oxygen α-proton), 3.48 (4H, t, *J* = 9.0 Hz), 1.93 (4H, q, *J* = 6.0 Hz, Br α-proton).

$^{13}\text{C-NMR}$ (300 MHz, $\text{DMSO-}d_6$) δ (ppm): 157.2, 144.2, 139.7, 136.2, 132.4, 131.2, 128.2, 126.7, 114.2, 64.8, 48.1, 28.5.

ESI-HRMS= Chemical Formula: $\text{C}_{32}\text{H}_{30}\text{N}_6\text{NaO}_2$, Measured (M/Z): 553.2324. Calculated (M/Z) = 553.2322 $[\text{M}+\text{Na}]^+$

Synthesis of 4,4'-(cyclopent-1-ene-1,2-diyl)bis(5-methylthiophene-2-carbaldehyde) (1-3). Compound 1,2-bis(5-chloro-2-methylthiophen-3-yl)cyclopent-1-ene (1-2) (5.5 g, 1 eq.) was charged into the cleaned dry 500 mL three necked round bottom flask with the addition of dry ethyl ether (200 mL) at room temperature under N_2 gas atmosphere. The reaction mixture cooled to -30 to -40°C and stirred for 10 min. After that, $n\text{-BuLi}$ (20 mL, 3 eq.) was added into the above reaction mixture under N_2 gas atmosphere by syringe very carefully and slowly about 20 to 30 min at -30 to -40°C and allowed to stir for 30 minute at the same temperature. Then, the reaction mixture was allowed to stir at room temperature until the reaction mixture color became dark brown, followed by the addition of dry DMF (4 mL, 3 eq.) into reaction mixture at room temperature very slowly within 10-15 minutes and stirred for additionally 3hr. The progress of the reaction was monitored by TLC. After completion, the reaction mixture was quenched by adding H_2O (10 mL) and stirred for 20 min. The organic layer was separated, washed with H_2O (200 mL x 2) and brine solution (200 mL x 2) and dried over MgSO_4 , filtered and evaporated to dryness. The crude residue of desired intermediate 1-3 was subjected to column chromatography (silica gel, hexane/ethyl acetate: 8/2 for 1-3). Light greenish color solid desired intermediate 1-3 was recovered (Desired yield = 2.5 g, 48% w/w)

$^1\text{H-NMR}$ (300 MHz, CDCl_3) δ (ppm): 9.74 (2H, s), 7.43 (2H, s), 2.83 (4H, t, $J = 7.5$ Hz), 2.15–2.10 (2H, m), 2.05 (6H, s).

$^{13}\text{C-NMR}$ (300 MHz, CDCl_3) δ (ppm): 182.3, 146.3, 140.2, 137.3, 137.0, 135.0, 38.4, 22.9, 15.3.

ESI-HRMS= Chemical Formula: $\text{C}_{17}\text{H}_{17}\text{O}_2\text{S}_2$, Measured (M/Z): 317.0664. Calculated (M/Z) = 317.0668 $[\text{M}+\text{H}]^+$.

Synthesis of 4,4'-(cyclopent-1-ene-1,2-diyl)bis(5-methylthiophene-4,2-diyl)dimethanol (1-4). The desired intermediate 4,4'-(cyclopent-1-ene-1,2-diyl)bis(5-methylthiophene-2-carbaldehyde) (1-3) (2.5 g, 1 eq.) was charged into the cleaned dry 250 mL three necked round bottom flask with the addition of dry MeOH: DCM (75:75 mL, 1:1 ratio) at room temperature under N_2 gas atmosphere. The reaction mixture was cooled to 0°C and stirred for 10 minute. After that, NaBH_4 (0.747 g, 2.5 eq.) was added into the above reaction mixture portion wise very slowly about 10 min at 0°C under N_2 gas atmosphere and allowed to stir for 4 hr. The progress of the reaction was monitored by TLC. After completion, the reaction mixture was quenched by adding H_2O (5 mL) and stirred for 10 min. The organic layer was separated, washed with H_2O (200 mL) and brine solution (200 mL) and dried over MgSO_4 , filtered and evaporated to dryness. The crude residue was subjected to column chromatography (silica gel, hexane/ethyl acetate: 9/1 to 6/4). A light brown color liquid of desired intermediate 1-4 was recovered (Desired yield = 2.3 g, 90% w/w).

$^1\text{H-NMR}$ (300 MHz, CDCl_3) δ (ppm): 6.66 (2H, s), 4.68 (4H, s), 2.76 (4H, t, $J = 7.5$ Hz), 2.07–2.04 (2H, m), 1.96 (6H, s).

$^{13}\text{C-NMR}$ (300 MHz, CDCl_3) δ (ppm): 136.2, 135.4, 134.5, 65.5, 38.5, 23.0, 14.5.

Synthesis of 1,2-bis(2-methyl-5-((prop-2-yn-1-yloxy)methyl)thiophen-3-yl)cyclopent-1-ene (1-5). Compound (4,4'-(cyclopent-1-ene-1,2-diyl)bis(5-methylthiophene-4,2-diyl)dimethanol (1-4) (2.0 g, 1 eq.) was charged into a cleaned dry 100 mL three necked round bottom flask at room temperature under nitrogen gas atmosphere followed by the addition of dry DMF (100 mL) through syringe into reaction mixture and nitrogen gas was further purged for 15 min. Strong base NaH (0.6 g, 4 eq.) was then added gradually to the reaction mixture (over 10 minutes) followed by the addition of imidazole (0.21 g, 0.5 eq.) with continuous stirring for 15-20 min until the reaction color turned to yellowish and left at room temperature. Then, the propargyl bromide (2.36 mL, 5 eq.) was added drop-wise into reaction mixture and allowed to stir for overnight. The reaction was monitored by TLC. On completion, reaction was quenched by crushed ice. Reaction mixture was then extracted with diethyl ether (200 mL). The Diethyl ether organic layer was separated out and washed with H_2O (2 x 100 mL) followed by utilizing brine solution (2 x 100 mL) and collected organic layer dried over MgSO_4 . Filtered organic layer was evaporated under reduced pressure and the crude residue obtained was subjected to column chromatography (silica gel, Hexane/EtOAc: 9/1 for 1-5). Light brownish color liquid of desired intermediate 1-5 was recovered (Desired yield = 1.5 g, 60% w/w).

$^1\text{H-NMR}$ (300 MHz, CDCl_3) δ (ppm): 6.67 (2H, s), 4.61 (4H, s), 4.09 (4H, d, $J = 2.4$ Hz), 2.73 (4H, t, $J = 7.2$ Hz), 2.44 (2H, s, $J = 2.4$ Hz), 2.04–1.99 (2H, m), 1.92 (6H, s).

$^{13}\text{C-NMR}$ (300 MHz, CDCl_3) δ (ppm): 135.8, 135.3, 135.0, 134.6, 128.8, 79.5, 74.7, 65.6, 56.0, 38.3, 23.0, 14.3.

ESI-HRMS= Chemical Formula: $\text{C}_{23}\text{H}_{24}\text{NaO}_2\text{S}_2$, Measured (M/Z): 419.1110. Calculated (M/Z) = 419.1112 $[\text{M}+\text{Na}]^+$

Synthetic procedure of polymer (P-PHT)

Compounds 1,2-bis(2-methyl-5-((prop-2-yn-1-yloxy)methyl)thiophen-3-yl)cyclopent-1-ene (1-5) (0.5 g, 1 eq.), 1,2-bis(4-(3-azidopropoxy)phenyl)-1,2-diphenylethene (2-3) (0.66 g, 1 eq.) and $\text{Cu}(\text{PPh}_3)_3\text{Br}$ (1.17 g, 1 eq.) were charged into a cleaned dry 100 mL three necked round bottom flask at room temperature, followed by the addition of dry DMF (20 mL) through syringe into reaction mixture and nitrogen gas was further purged for 15 min. After that, the reaction mixture was allowed to reflux at 80°C and stirred for 4 days. Then reaction mixture was cooled to room temperature, diluted with DMF (5 mL), added into the 500 mL THF/Hexane (1:20) and after 5 min stirring precipitate out which collected by filtration, dried at 40°C to desired polymer P-PHT (Desired yield = 0.4 g, 42%).

GPC results: $M_w = 11634$ g/mol, $M_n = 7489$ g/mol, $\text{PDI} = 1.53$

$^1\text{H-NMR}$ (300 MHz, CDCl_3) δ (ppm): 7.53 (2H, br), 7.05-6.99 (14H, m), 6.90 (2H, br), 6.65-6.59 (4H, m), 4.58 (12H, br), 3.88 (4H, br), 2.73 (4H, br), 2.32 (4H, br), 2.03-2.01 (2H, m), 1.92 (6H, br).

$^{13}\text{C-NMR}$ (300 MHz, CDCl_3) δ (ppm): 156.2, 144.2, 139.7, 136.9, 135.8, 135.7, 135.3, 134.6, 132.6, 131.4, 127.8, 127.6, 126.3, 113.7, 67.0, 64.0, 47.3, 38.4, 30.1, 23.0, 14.4.

3. Results and discussion

Design and synthesis

The designed photo-switchable polymer (**P-PHT**) is composed of diarylethene (DAE) and tetraphenylethene (TPE) moieties along with a protonable triazole linker as its repeating unit. The cyclized DAE unit after UV-irradiation adopts a more planar and rigid core but pushes the bulky methyl group out of the core plane, which results in intermolecular steric hindrance among cyclized DAE units in the whole molecular assembly. Therefore, such events of intermolecular repulsions among cyclized DAE units are supposed to be associated with the tuning of AIE behaviour in **P-PHT**. Moreover, the protonable triazoles in **P-PHT** with their cation characteristics under acidic conditions might be useful to explore further insights into the findings.

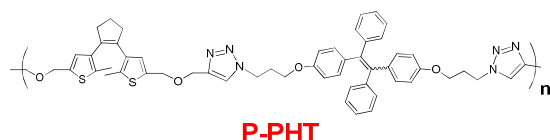


Chart 1. Structure of **P-PHT**.

The synthetic route to obtain polymer **P-PHT** is shown in Scheme 1. Commercially available starting compound (2-chloro-5-methylthiophene) has been used to obtain the intermediate **1-1**^{67,68} by employing Friedel-Crafts Acylation reaction condition and intermediate **1-2** obtained through McMurry reaction condition. After that, *n*-BuLi chemistry was employed to get intermediate **1-3** with a new synthetic method and the desirable yield, then the terminal ends of alcohol intermediate **1-4** were generated via reducing agent NaBH₄ and alkyne terminated intermediate **1-5** was obtained in the presence of NaH, Imidazole and propargyl bromide in DMF at ambient temperature, which were further reacted with azide terminated TPE-based intermediate **2-3**³⁸ via Cu(I) catalyzed click reaction to obtain **P-PHT** (open).⁶⁹ Intermediate **2-3** was successfully synthesized in our previous report and carried out in this study.

Photo-switching behavior of DAE in organic solvent media (THF)

The optical property of polymer **P-PHT** was first measured in THF. As demonstrated in Fig. 1(a), upon UV-irradiation the open-form of **P-PHT** was optically switched to its close-form, i.e., from **P-PHT** (open) to **P-PHT** (close). As summarized in Fig. 1, the UV/Vis and photoluminescence (PL) spectral changes of **P-PHT** (10 μM) after UV-irradiation (40 min and λ = 346 nm) and the saturation time was monitored in Fig. S1. The UV-Vis spectrum of **P-PHT** (open) exhibited absorption bands at 245 nm (*n*-π* transition of DAE) and 328 nm (π-π* transition of TPE unit), see Fig. 1(b). After UV-irradiation, **P-PHT** (close) illustrated an enhanced absorption band at 245 nm and a blue-shifted absorption shoulder at 308 nm. Due to the formation of cyclized conformation of DAE in **P-PHT** (close),⁷⁰ we also observed a broad and less intense absorption band at 544 nm, which is shown in the inset of Fig. 1(b). Under similar conditions in Fig. 1(c), the PL spectrum of **P-PHT** (close) after

UV-irradiation exhibited monomeric emission band at λ_{max} = 385 nm (with a quantum yield = 19% for **P-PHT** (close) in THF solvent media by using a pyrene standard), which belonged to the monomeric emission of TPE.^{57,58} The higher monomeric emission of **P-PHT** in the close form rather than the open form was observed in THF due to a more planar and rigid structure of the cyclized DAE unit upon UV-irradiation,⁷¹ where the free rotations of the ethene moiety and aryl groups were restricted to induce the steric hindrance with larger separations and less π-π interactions among TPE.

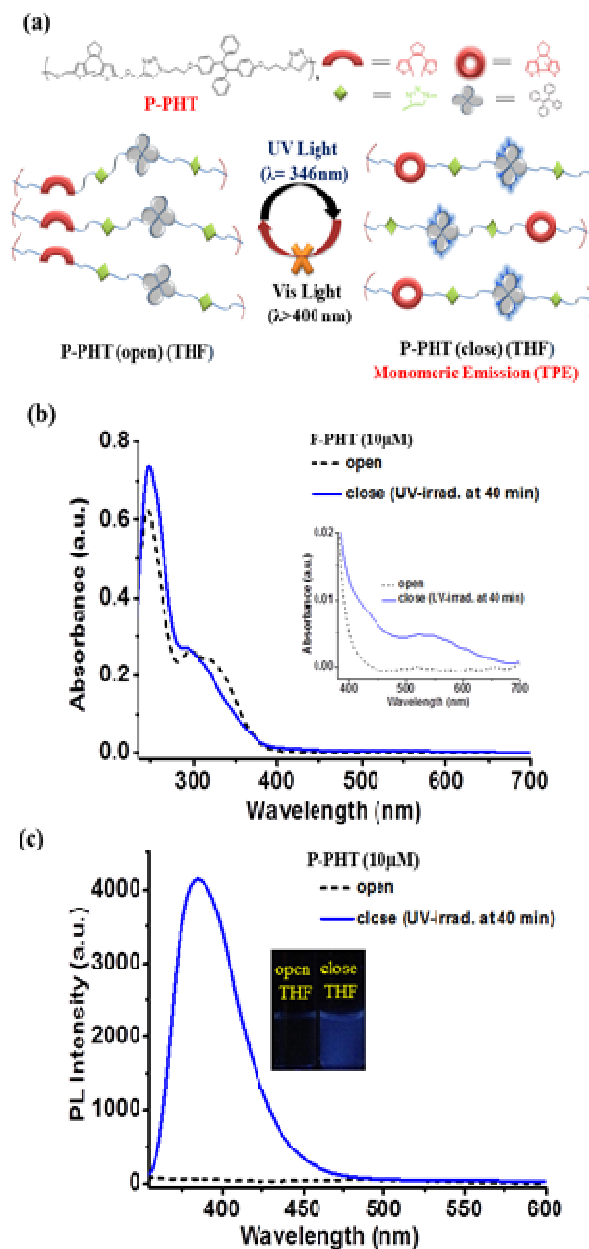


Fig.1 **P-PHT** in THF before and after UV-irradiation, (a) Pictorial diagram of **P-PHT** (open to close). (b) UV-Vis spectral changes of **P-PHT** (open to close). (c) PL spectral changes of **P-PHT** (open to close). Inset: Photoimages of **P-PHT** at 0 min and 40 min. (λ_{ex} = 320 nm for PL exp.)

Under similar experimental conditions (Fig. 1), we have performed new control experiments to study the accessibility of such monomeric emission band at $\lambda_{\max} = 385$ nm by taking into account of DAE intermediate, such as compound **1-5** and corresponding UV-Vis and PL spectral changes are monitored and summarized in Fig. S2. After UV-irradiation, a slight increase of absorption band at 241 nm in compound **1-5** was observed. Due to the formation of cyclized conformation of DAE in compound **1-5** (close), we also observed a broad and less intense absorption band at 455 nm in Fig S2(a). Under similar conditions, the PL spectrum of compound **1-5** (close) after UV-irradiation illustrated none of the monomeric emission band at $\lambda_{\max} = 385$ nm was observed in Fig. S2(b). Thus, DAE unit itself alone cannot generate the monomeric emission in organic solvent media (THF) under UV-irradiation. Therefore, the emission peak at $\lambda_{\max} = 385$ nm is belongs to the monomeric emission of TPE in **P-PHT** upon UV-irradiation. However, the irradiation of visible light ($\lambda > 400$ nm) on **P-PHT** (close) was irreversible towards its original open-form. Since DAEs in polymer backbone adopt anti-parallel conformation and thus to enhance the efficiency of cyclizations on DAEs (close) up to 100%.⁷² Therefore, the incorporation of DAEs without any extended conjugation in polymer backbone as the part of repeating unit is an interesting and unique case. Furthermore, the cyclization events of DAEs to cause their bulkier alkyl substituents out of plane with respect to DAE rigid cores might enforce polymer backbones to adopt more favorable and stable conformations,⁷¹ which also resisted cycloreversions of DAEs with intact and unique monomeric emissions of TPEs. It demonstrates that the substituents exerting a +M effect on the reactive carbon atoms, e.g. methoxy groups⁷³ or fluorine atoms,⁷⁴ significantly stabilize the ring-closed isomers resulting in marked decreases of quantum yields for ring opening. On the contrary, the electron-withdrawing cyano groups attached to reactive carbon atoms on DAEs accelerate the photochemical cycloreversion with high quantum yields.⁷⁵ Moreover, the lack of any electron withdrawing substituents (such as cyano groups and fluoro atoms) on DAEs in our system induce irreversibility.^{70,76} Interestingly, the photo-irreversibility of DAEs is advantageous and especially desired for the optical memory use, where many-time readouts without erasing memory can be achieved.⁷⁷⁻⁷⁹ With the presence of the protonable triazole linker, we further explored the photo-switching behaviour by UV exposure of DAE in **P-PHT** (10 μM in THF) under an acidic condition (HCl 100 eq.). Similar to the previous photo-switching behaviour of **P-PHT** without HCl, the PL spectrum in Fig. S3 showed a comparable pattern but illustrated a shorter UV-switching time (from open to close for m) of 20 min with HCl in contrast to 40 min without HCl. Therefore, under the acidic condition (HCl 100 eq.) the photo-switching behaviour of **P-PHT** with the protonable triazole was further activated in THF. The irradiation of visible light ($\lambda > 400$ nm) on **P-PHT** (close) was also irreversible even under the acidic condition. In addition, we have performed the chemical stability experiment of **P-PHT** (close) under acidic condition (HCl 100 eq. in THF, at different time intervals from 0 to 24 hr) in Fig. S4, where none

of the further intensity increments or decrements of monomeric emissions of TPE were observed. Therefore, our experimental results revealed a quite higher chemical stability of **P-PHT** under acidic condition.

Furthermore, we also explored the structural conformation changes of DAE moiety in **P-PHT** via $^1\text{H-NMR}$ spectroscopy in Fig. 2. From the $^1\text{H-NMR}$ spectra of **P-PHT**(open) and **P-PHT**(close) in Fig. 2, the chemical shift of the methyl proton ($-\text{CH}_3$ group) on thiophene ring of DAE in **P-PHT** (open) is located at 1.92 ppm and for photo-cyclized DAE in **P-PHT** the methyl proton ($-\text{CH}_3$ group) was slightly shifted to up-field at 1.90 ppm. Generally, the ^1H NMR of polymers are broaden but still we can observed the noticeable changes in the close form of DAE in **P-PHT** (changed from 1.70 to 2.75 ppm), which further confirmed the structural changes before and after UV-irradiation. Since the chemical shifts of methyl protons ($-\text{CH}_3$ group) on thiophene rings of DAEs vary according to the structural design, some reports demonstrate chemical shifts up to 0.04 ppm in small molecular systems.^{80,81} However, CH_3 protons in our polymer **P-PHT** exhibited broad $^1\text{H-NMR}$ pattern and thus to induce a less chemical shift (0.02 ppm up field). Moreover, CH_2 protons on cyclopentenenes ring of DAE exhibited the chemical shift difference of 0.03 ppm (i.e., from 2.743 ppm to 2.713 ppm), where the integrated areas indicated a 100% conversion of **P-PHT** (open) to **P-PHT** (close).

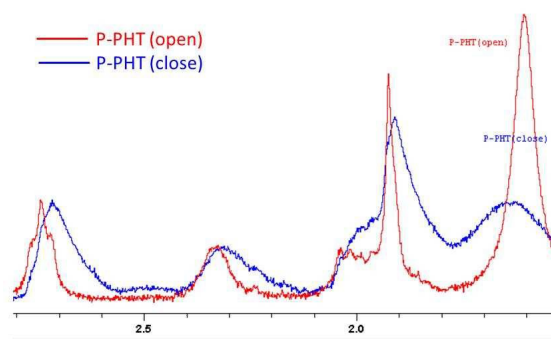


Fig. 2 $^1\text{H-NMR}$ of **P-PHT** (6 mg in CDCl_3) before and after UV-irradiation (at $\lambda = 346$ nm for 40 min).

AIE emissions in semi-aqueous media

As illustrated in Fig. 3(a), upon adding water to **P-PHT** (open) in THF the AIE behaviour was introduced due to the restriction of intra-molecular rotation of phenyl ring and significant UV-Vis and PL spectral changes of **P-PHT** were observed and summarized in Figs. S5 and 3(b), respectively. As shown in Fig. 3(c), by increasing the water content in **P-PHT** (open), the AIE emission at $\lambda_{\max} = 480$ nm was gradually enhanced at 20-80% H_2O due to the formation of self-assembly among TPE units. However, the AIE emission of **P-PHT** (open) was blue-shifted to $\lambda_{\max} = 466$ nm over 90% H_2O (quantum yield = 20% for **P-PHT** (open) at 90% water content by using quinine hemisulfate standard and molar absorption coefficient ($E = 21,700 \text{ L mol}^{-1} \text{ cm}^{-1}$), due to the formation of higher aggregation of TPE. However, as shown in Figs. 3(b) and 3(c) the AIE intensity was suppressed with over-supply of water content up to 100% in

contrast to 90% H₂O. Therefore, the maximum AIE at 90% H₂O was utilized for the rest of experiments, where AIE behavior will be examined for the energy transfer from TPE to DAE in P-PHT. Moreover, the related absorption bands of DAE (245 nm) and TPE (328 nm) of P-PHT (open) at high water contents (over 80%) in Fig. S5 were red-shifted to 251 and 354 nm, respectively, which further confirmed the aggregation of TPE.

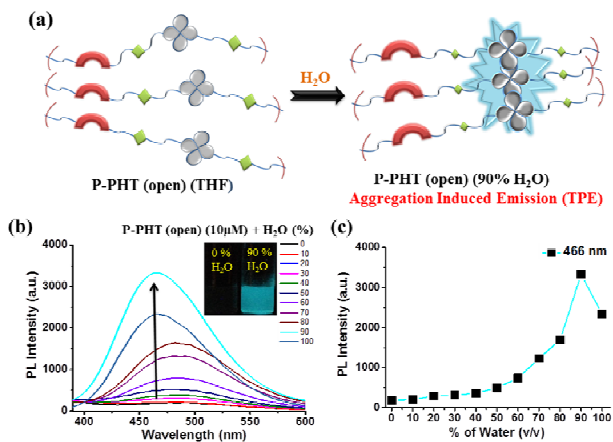


Fig. 3 (a) Pictorial diagram of P-PHT (open only) by increasing water contents. (b) PL spectral changes of P-PHT (open) in THF by increasing water contents. Inset: Photoimages of P-PHT (open) at 0 and 100% water contents. (c) Maximum PL intensities of P-PHT (open) by increasing water contents. ($\lambda_{\text{exc}} = 320$ nm for PL exp.)

Photo-switching behavior of DAE in semi-aqueous media

Compared with P-PHT (open) by adding water in Fig. 3, the AIE

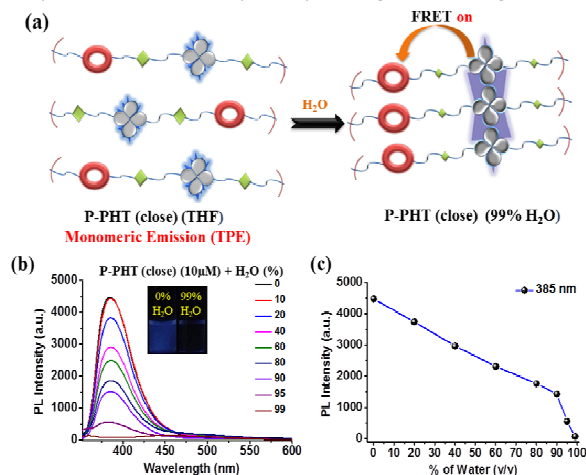


Fig. 4 (a) Pictorial diagram of UV-irradiated P-PHT (close) at different water contents (0 and 99% H₂O). (b) PL spectra of P-PHT (close) at 0 and 99% water contents. Inset: Photoimages of P-PHT (close) at corresponding water contents. (c) Maximum PL intensities of P-PHT (close) by increasing water contents. ($\lambda_{\text{exc}} = 320$ nm for PL exp.)

behaviour of the close form in P-PHT (by UV-irradiation at $\lambda = 346$ nm for 40 min) was also studied in various aqueous conditions (0 and 99% H₂O) as shown in Fig. 4(a). The corresponding PL spectral changes are summarized in Fig. 4(b),

where the monomeric emission (without AIE emission of TPE) of P-PHT (close) was gradually quenched up to 99% H₂O. As illustrated in Fig. 4 (b), due to the Förster resonance energy transfer (FRET) from TPE (donor) to the cyclized DAE unit (acceptor) the AIE emission of TPE was totally prohibited even with high water contents in P-PHT (close) in contrast to P-PHT (open) at 90% H₂O in Fig. 3. Hence, the monomeric emission (without AIE emission of TPE) of P-PHT (close) was gradually quenched in Fig. 4 (c) owing to the π - π stacking of TPE by increasing the water contents (0 to 99% H₂O).

Since we have studied the AIE behaviour of P-PHT (open and close) upon adding water in Fig. 3 and 4, we also performed other comparative experiments of P-PHT at 90% water content before and after UV-irradiation as illustrated in Fig. 5(a).

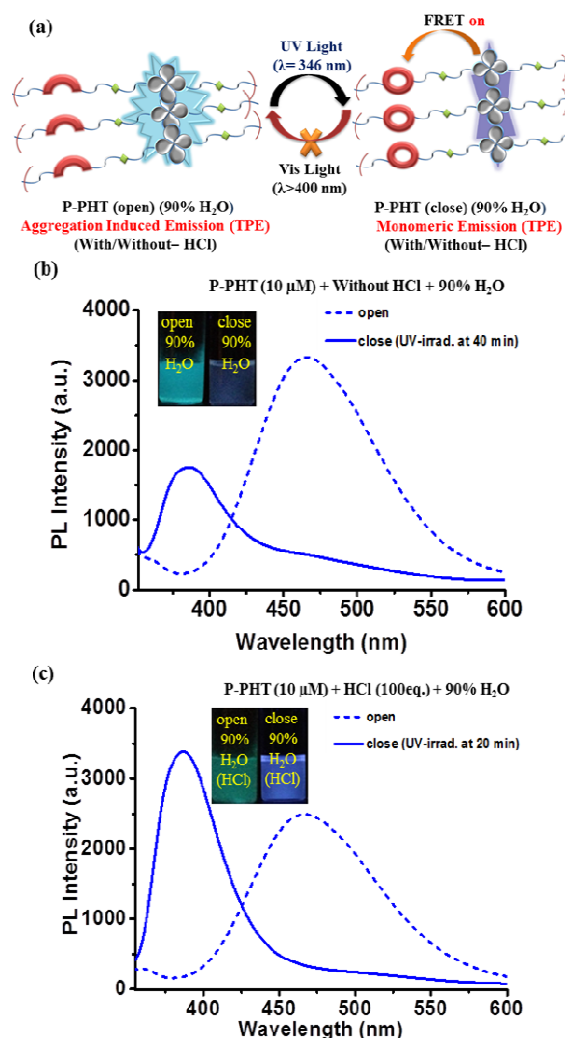


Fig. 5 P-PHT at 90% water content before and after UV-irradiation (at $\lambda = 346$ nm), (a) Pictorial diagram of P-PHT (90% H₂O) from open to close form upon UV-irradiation. (b) and (c) PL spectral changes of P-PHT with HCl (100eq.), respectively. Insets: Photoimages of P-PHT (90% H₂O) at 0, 40 min (UV-irradiation) without HCl and at 0, 20 min (UV-irradiation) with HCl, respectively. ($\lambda_{\text{exc}} = 320$ nm for PL exp.)

The corresponding PL spectral changes without and with HCl (100eq.) are summarized in Figs. 5(b) and 5(c), respectively. In addition, the gradual PL saturation emissions for the ring closure of DAE after different UV-irradiation time intervals are displayed in Fig. S6.

Interestingly, upon UV-irradiation (at $\lambda = 346$ nm for 40 min) of **P-PHT** (open) at 90% water content, the AIE emission of TPE at $\lambda_{\max} = 466$ nm was gradually quenched and emission band at $\lambda_{\max} = 385$ nm were simultaneously enhanced in Fig. 5(b). Therefore, regardless of high water contents done after or before UV-irradiation, the similar results of UV exposure to induce only monomeric emissions (without AIE) were observed in Figs. 4 and 5, respectively. Thus, the AIE emission of **P-PHT** (open) was quenched due to the efficient energy transfer from TPE to the cyclized DAE unit, because an emitting chromophore could be quenched by the nearby cyclized DAE unit (as an acceptor) to release energy via non-radiative transition.⁷⁰ In addition, to fulfil the requirement of FRET between the TPE (donor) and photo-switchable unit DAE (acceptor) in **P-PHT**, the maximum overlap of the AIE emission of TPE and the absorption of the cyclized DAE fully supported the occurrence energy transfer event in **P-PHT** (close) of Fig. S7. Interestingly, the monomeric emission of **P-PHT** (close) was originated from TPE still existed in the AIE favorable condition (even at 90% water content). Therefore, we believe that the more planar and rigid structure of the cyclized DAE unit under UV-irradiation induced the steric hindrance with larger separations and less π - π interactions among TPE in **P-PHT** (close). Moreover, the monomeric emission (at $\lambda_{\max} = 385$ nm) of TPE of **P-PHT** (close) in 90% water content in Fig. 5(b) was reduced by the larger aggregation of TPE in H₂O in comparison with the monomeric emission of TPE of **P-PHT** (close form in THF) in Fig. 1(c). Under similar experimental conditions (i.e., Fig. 5(b)), we also performed another control experiment to investigate the accessibility of monomeric emission (at $\lambda_{\max} = 385$ nm) of TPE with intermediate **2-3** after UV-irradiation (40 min at $\lambda = 346$ nm) at 90% water content as illustrated in Fig. S8. Upon UV-irradiation, no any further changes in the intensity of AIE emission for TPE were observed and none of the monomeric emission (at $\lambda_{\max} = 385$ nm) could be noticed in intermediate **2-3** in Fig. S8. Therefore, TPE unit itself alone cannot generate the monomeric emission in AIE favorable conditions (at 90% water content) under UV-irradiation.

Similarly, we also explored the PL spectral changes in Fig. 5(c) and the AIE behaviour by UV-irradiation of **P-PHT** (90% H₂O) under an acidic condition (HCl 100 eq.) and the saturation time is illustrated in Fig. S6(b), where the AIE emission (at $\lambda_{\max} = 466$ nm) of TPE (with a quantum yield = 15% for **P-PHT** (open) at 90% water content under acidic condition (HCl 100eq.) by using a quinone hemisulfate standard) was slightly reduced due to the presence of electrostatic repulsion among protonated triazole in **P-PHT** (open). After UV-irradiation, the AIE of TPE (at $\lambda_{\max} = 466$ nm) was diminished completely in Fig. 5(c) but obtained two-fold higher monomeric emission of TPE. Moreover, the two-fold monomeric emission of TPE (at $\lambda_{\max} = 385$ nm) of **P-PHT** (close) under the acidic condition in 90% water content as shown in Fig. 5(c) was improved by the

protonation of triazole to induce less π - π stacking and larger separation of TPE, which became comparable with the larger monomeric emission of TPE (at 385 nm) of **P-PHT** (close) in THF as shown in Fig. 1(c). Simultaneously, the AIE of TPE with HCl in Fig. 5(c) was completely quenched in a shorter UV-switching time (from open to close form) of 20 min with HCl in contrast to 40 min without HCl in Fig. 5(b), which might be due to the protonable triazole was further separated under the acidic condition to induce larger separation and easier photocyclization of DAE. Therefore, the photo-switching behaviour of DAE in **P-PHT** with the protonable triazole under the acidic condition was further stimulated with larger separations and less π - π interactions among TPE at 90% water content.

Study of photo-switchable polymer (**P-PHT**) by time-resolved photoluminescence (TRPL)

The fluorescence lifetime values of polymer **P-PHT** before and after UV-irradiation with/without HCl (100 eq.) at 90% water content are summarized in Fig. 6.

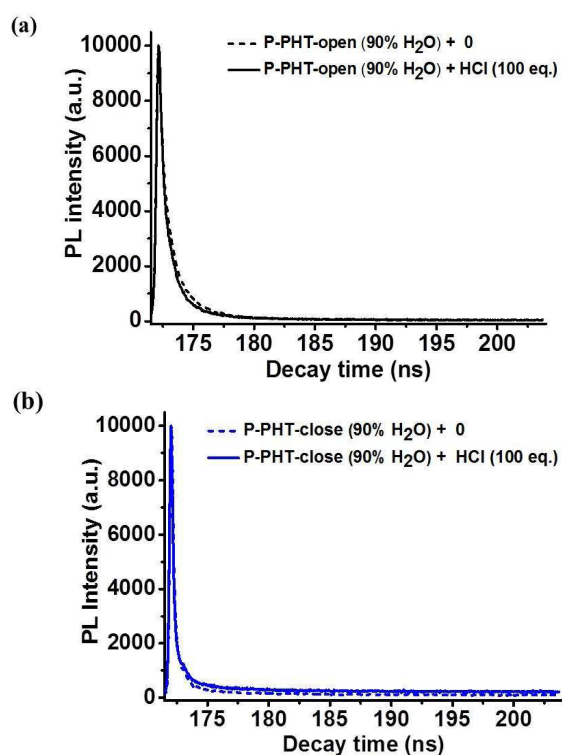


Fig. 6 (a) Before UV-irradiation, time-resolved fluorescence of polymer **P-PHT** (open) of AIE emissions (at $\lambda_{\max} = 466$ nm) with/without HCl (100eq.). (b) After UV-irradiation, time-resolved fluorescence of polymer **P-PHT** (close) of monomeric emissions (at $\lambda_{\max} = 385$ nm) with/without HCl (100eq.).

Before UV-irradiation, the fluorescence lifetime of AIE emission (at $\lambda_{\max} = 466$ nm) in **P-PHT** (open) at 90% water content without HCl (100 eq.) was $\tau = 1.80$ ns, whereas in the presence of HCl (100 eq.), the fluorescence lifetime of AIE emission was slightly decreased to $\tau = 1.54$ ns in contrast to without HCl in Fig. 6(a). Therefore, the decrease of the

fluorescence lifetime for AIE emission in **P-PHT** (open) under an acidic condition (HCl 100 eq.) is further validated our findings in Fig. 5(c). After UV-irradiation, the fluorescence lifetime of monomeric emission (at $\lambda_{\max} = 385$ nm) in **P-PHT** (close) at 90% water content without HCl (100 eq.) was $\tau = 1.16$ ns, whereas in the presence of HCl (100 eq.), the fluorescence lifetime monomeric emission in **P-PHT** (close) was slightly increased to $\tau = 1.29$ ns in Fig. 6(b). Thus, the increase in the fluorescence lifetime of monomeric emission **P-PHT** (close) under an acidic condition (HCl 100 eq.) supports our results of the photo-switching behaviour for DAE in **P-PHT** with the protonable triazole under the acidic condition, which was further stimulated at 90% water content in Fig. 5(c).

Aggregation states of photo-switchable polymer (**P-PHT**) in semi-aqueous media

The AIE behavior of TPE in **P-PHT** (open and close forms by UV-irradiation at $\lambda = 346$ nm for 40 min) was further explored by the scanning electron microscopy (SEM) in the absence and presence of water (i.e., 0% and 90%) as shown in Fig. S9(a)-S9(c). Before UV-irradiation, the morphological patterns of **P-PHT** (open) in THF at 0% and 90% of water exhibited uniform and nano-spherical aggregates in Figs. S9(a) and S9(b), respectively and thus AIE of TPE in **P-PHT** (open) was verified. After UV-irradiation, the morphological pattern of **P-PHT** (close) in THF at 90% of water content caused diminished nano-spherical aggregates, which further validated the energy transfer event from TPE to DAE as shown in Fig. S9(c).

Under similar conditions, the aggregation behaviors of **P-PHT** (open and close form under UV-irradiation) in THF solution with various water contents were further verified by dynamic light scattering (DLS) experiments and illustrated in Figs. 7(a) and 7(b), respectively.

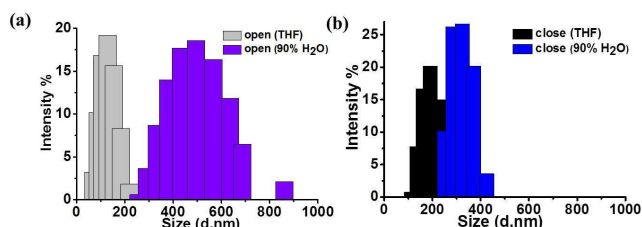


Fig. 7 DLS measurements of (a) **P-PHT** (open) in THF (i.e., 0%) and at 90% water content. Upon UV-irradiation, (b) **P-PHT** (close) in THF (i.e., 0%) and **P-PHT** (close) at 90% water content.

Before UV-irradiation in Fig. 7(a), **P-PHT** (open) in THF with 0% and 90% of water revealed aggregates mean sizes of 164 and 458 nm, respectively. After UV-irradiation (at $\lambda = 346$ nm for 40 min), **P-PHT** (close) in THF revealed slightly larger aggregates with the mean size of 255 nm in Fig. 7(b). Whereas, upon similar UV-irradiation the aggregates of **P-PHT** (close) at 90% of water content were significantly reduced to the mean size of 295 nm in Fig. 7(b). Therefore, the optical events and respective morphological patterns are further verified by DLS experiments.

Theoretical calculations of photo-switchable polymer (**P-PHT**)

Furthermore, to understand more about the molecular structure and associated properties of **P-PHT**, we performed theoretical studies, including density functional theory (DFT) and time-dependent DFT (TDDFT),⁸² by taking **PH-T** as a model compound in THF. It has been reported that the DAE unit with a carbon distance less than 4.2 Å is responsible for the photochromism,⁸³ so the carbon distance of the DAE unit in **PH-T** needs to be verified theoretically. Thus, the geometrical parameters of **PH-T** revealed the suitable bond lengths (<4.2 Å) of separated C-atoms in both open and close forms of DAE to be 3.676 and 1.544 Å, respectively. The optimized open and close structures of **PH-T** (before and after UV-irradiation) are demonstrated in Fig. 8(a) and their respective highest occupied molecular orbital (HOMO) and the lowest unoccupied molecular orbital (LUMO) levels are also illustrated in Figs. 8(b) and 8(c).

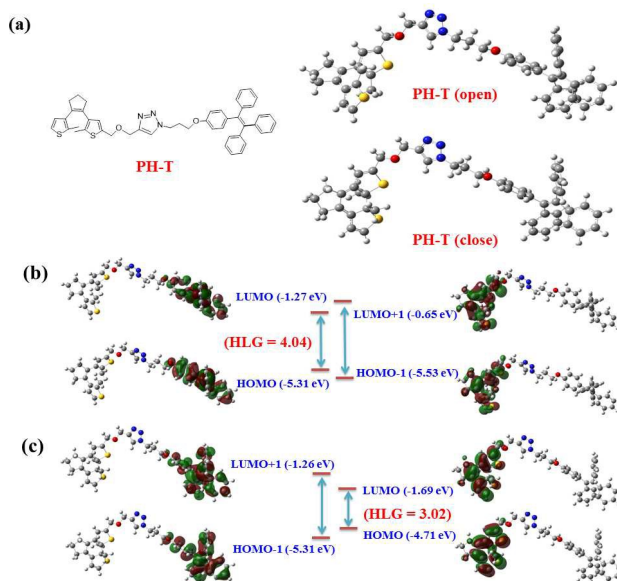


Fig. 8 (a) Geometries of optimized structures of **PH-T** (open and close forms). Frontier molecular orbital distributions of HOMO, LUMO, HOMO-1 and LUMO+1 iso-surfaces along with the energy eigen values in (eV), UV-Vis studies (b) **PH-T** (open) (c) **PH-T** (close) calculated at B3LYP/6-31G(d,p) level.

Before and after UV-irradiations of **PH-T** (open and close forms), the HOMO and LUMO levels were exactly located on the TPE in Fig. 8(b) and cyclized DAE unit in Fig. 8(c), respectively. Moreover, due to UV-irradiations the locations of HOMO and LUMO, along with HOMO-1 and LUMO+1, were completely reversed in Figs. 8(b) and 8(c). According to the theoretical results, the HOMO-LUMO bandgap of **PH-T** (close) was quite smaller as compared with HOMO-LUMO bandgap of **PH-T** (open), which is mainly due to the occurrence of energy transfer from TPE to DAE units. Therefore, the energy transfer event from TPE to DAE in **P-PHT** (close) was theoretically validated. Furthermore, the calculated transitions in UV-Vis spectral details of **PH-T** (from open to close form) at their minima and their main contributions to the first excitation are

summarized in Table S10. The theoretically calculated transitions in the UV-Vis of **P-PHT** (before and after UV-irradiation) were almost quite similar as observed experimentally.

Photo-switching behavior of DAE in solid films

In general, the isomerization from open to close forms of DAE in both solutions and solid films are quite common because of relatively small structural changes.⁷¹ In addition, TPE-based materials exhibit enhanced emission intensities in solid films as read out signals.⁴⁶ Moreover, to study the photo-switching behaviour of DAE with the combination of TPE unit into polymer **P-PHT** on solid films would be interesting. Therefore, both UV/Vis and PL spectral changes of **P-PHT** (before and after UV-irradiation) on uniform solid films of glass plate without and with HCl (100 eq.) are summarized in Fig. 9 and S11, respectively.

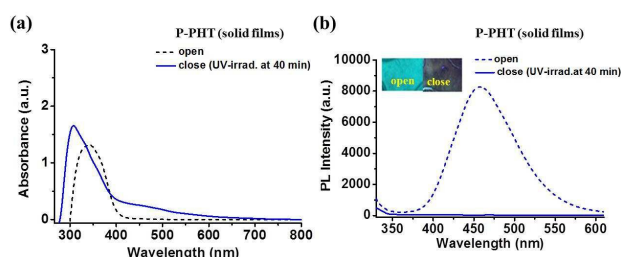


Fig. 9 **P-PHT** in solid films before and after UV-irradiation, (a) UV-Vis spectral changes of **P-PHT** (open to close). (b) PL spectral changes of **P-PHT** (open to close). Inset: Photoimages of **P-PHT** at 0 min and 40 min. ($\lambda_{\text{ex}} = 320$ nm for PL exp.)

Before UV-irradiation, UV-Vis spectra of **P-PHT** (open) in neat solid films exhibited broad absorption band at 345 nm in Fig. 9(a), due to the π - π stacking of TPE. After UV-irradiation (at $\lambda = 346$ nm for 40 min), the absorption peak at $\lambda_{\text{max}} = 345$ nm were completely quenched. Due to the cyclization events of DAE in **P-PHT** (close), a new and more intense absorption band in Fig. 9(a) appeared at 313 nm along with broad and less intense absorption pattern from 400 to 550 nm. Therefore, we believe that little UV-Vis spectral change of **P-PHT** might be due to non-extended conjugation on DAEs into our systems. Under similar condition, PL spectra of **P-PHT** (open) in neat solid films exhibited prominent emission peaks at similar position 458 nm in Fig. 9(b), respectively, due to the π - π stacking of TPE. After UV-irradiation (at $\lambda = 346$ nm for 40 min), the emission peaks at $\lambda_{\text{max}} = 458$ nm were completely quenched. However, the monomeric emission of TPE (at $\lambda_{\text{max}} = 385$ nm) in **P-PHT** (close) could not be observed in neat solid films, which was because the separation of TPE could not be accessible in solid films as the monomeric emission of TPE obtained in solution. Under similar conditions, we also explored the PL spectral changes of the AIE behaviour by UV-irradiation of **P-PHT** (solid films) under an acidic condition (HCl 100 eq.) as illustrated in Fig. S8. After UV-irradiation of **P-PHT** in solid films, the AIE of TPE with HCl in Fig. S11(b) was completely quenched in a shorter UV-switching time of 20 min (from open to close form) in contrast to 40 min without HCl in

Fig. 8(b), which might be due to the protonable triazole was further separated under the acidic condition to induce less steric hindrance and easier photo-cyclization of DAE in solid films. Nonetheless, due to the large π - π stacking and serious aggregation of TPE in solid films the monomeric emission of TPE (at $\lambda_{\text{max}} = 385$ nm) in solid films of **P-PHT** (close) could not be improved by the protonation of triazole under the acidic condition as that happened in 90% water content in Fig. 4(c).

Likewise, we also performed the other comparative experiments of **P-PHT** by employing the polymethyl methacrylate (PMMA) matrix to further investigate the accessibility of monomeric emission in polymer blend film. Therefore, we prepared the solution of **P-PHT**:PMMA (10:90 wt. ratio) in DCM and drop coated on glass plates. The corresponding UV-Vis and PL spectral changes of **P-PHT** (before and after UV-irradiation) on PMMA matrix without and with HCl (100 eq.) are summarized in Figs. S12 and S13, respectively. After UV-irradiation in Fig. S12(b), the AIE emission of TPE at $\lambda_{\text{max}} = 458$ nm was completely quenched. Related UV/Vis spectral changes of **P-PHT**/PMMA polymer blend film by UV-irradiation, the broad absorption band at 358 nm was completely quenched due to the cyclization events of DAE in **P-PHT** (close), a new and more intense absorption band in Fig. S12(a) appeared at 315 nm. Additionally, the similar experimental results were observed under acidic condition in a shorter period of time in Figs. S13(a) and S13(b). However, the monomeric emission of TPE (at $\lambda_{\text{max}} = 385$ nm) in **P-PHT** (close) could not be observed in PMMA matrix and neat solid films, which was because the separation of TPE could not be accessible in solid films as the monomeric emission of TPE obtained in solution. Therefore, the phenomena of energy transfer from TPE to DAE in the close form of DAE in **P-PHT** (close) along with AIE of TPE in the open form of DAE in **P-PHT** (open) occurred in both solutions and solid films. Significantly, the disappearance of the monomeric emission of TPE (at $\lambda_{\text{max}} = 385$ nm) in solid films of **P-PHT** (close) was totally different from the result happened in solution, so this observation fully verify the occurrence of the monomeric emission of TPE (at $\lambda_{\text{max}} = 385$ nm) in the solution media of **P-PHT** (close) was due to the separation of TPE in the solution state.

4. Conclusions

In conclusion, the photo-switching behaviour of DAE (from open to close form under UV-irradiation) in **P-PHT** were prominent in organic solvent (THF), high water contents (at 90% H₂O) and solid films. The AIE behaviour of TPE in **P-PHT** (close) at 90% water content was quenched and special monomeric emissions were induced by efficient energy transfer from TPE to the cyclized DAE unit. Regardless of high water contents done after or before UV-irradiation, the similar results of UV exposure to induce only monomeric emissions (without AIE) were observed. Furthermore, the photo-switching behaviour of DAE in **P-PHT** with the protonable triazole under the acidic condition was further stimulated in both organic solvent (THF) and high water contents. Moreover, the experimental findings were fully validated by theoretical

ARTICLE

Journal Name

studies. However, the monomeric emission of TPE in **P-PHT** (close) could not be observed in solid films, because the separation of TPE could not be accessible in solid films as the monomeric emission of TPE obtained in solution. Hence, this observation fully verifies the occurrence of the monomeric emission of TPE in the solution media of **P-PHT** (close) was due to the separation of TPE in the solution state. Therefore, such photo-chromism events of **P-PHT** arouse significantly decreased AIE emissions and increased monomer emissions, which provided a new insight into the fluorescence of AIE compounds for future applications.

Acknowledgements

The financial supports of this project are provided by the Ministry of Science and Technology (MOST) in Taiwan through MOST 103-2113-M-009-018-MY3 and MOST 103-2221-E-009-215-MY3.

Notes and references

- 1 M. Szymanski, J. M. Beierle, H. A. V. Kistemaker, W. A. Velema and B. L. Feringa, *Chem. Rev.*, 2013, **113**, 6114–6178.
- 2 L. X. Yu, Y. Liu, S. C. Chen, Y. Guan and Y. Z. Wang, *Chin. Chem. Lett.*, 2014, **25**, 389–396.
- 3 M. Irie and K. Uchida, *Bull. Chem. Soc. Jpn.*, 1998, **71**, 985–996.
- 4 M. Irie, T. Lifka, S. Kobatake and N. Kato, *J. Am. Chem. Soc.*, 2000, **122**, 4871–4876.
- 5 C. Jia, A. Migliore, N. Xin, S. Huang, J. Wang, Q. Yang, S. Wang, H. Chen, D. Wang, B. Feng, Z. Liu, G. Zhang, D.H. Qu, H. Tian, M. A. Ratner, H. Q. Xu, A. Nitzan and X. Guo, *Science*, 2016, **352**, 1443–1445.
- 6 P. Wesenhagen, J. Areephong, T. F. Landaluce, N. Heureux, N. Katsoni, J. Hjelm, P. Rudolf, W. R. Browne and B. L. Feringa, *Langmuir*, 2008, **12**, 6334–6342.
- 7 S. Kobatake and M. Irie, *Bull. Chem. Soc. Jpn.*, 2004, **77**, 195–210.
- 8 E. Kim, Y. K. Choi and M. H. Lee, *Macromolecules*, 1999, **32**, 4855–4860.
- 9 W. Zhu, Y. Yang, R. Metivier, Q. Zhang, R. Guillot, Y. Xie, H. Tian and K. Nakatani, *Angew. Chem.*, 2011, **50**, 10986–10990.
- 10 M. Irie, *Jpn. J. Appl. Phys.*, 1989, **28**, 215–219.
- 11 T. Tsujioka, M. Kume and M. Irie, *Jpn. J. Appl. Phys., Part 1*, 1995, **34**, 6439–6443.
- 12 M. Irie, T. Fukaminato, T. Sasaki, N. Tamai and T. Kawai, *Nature*, 2002, **420**, 759–760.
- 13 T. Fukaminato, T. Sasaki, N. Tamai, T. Kawai and M. Irie, *J. Am. Chem. Soc.*, 2004, **126**, 14843–14849.
- 14 T. Fukaminato, T. Umamoto, Y. Iwata, S. Yokojima, M. Yoneyama, S. Nakamura and M. Irie, *J. Am. Chem. Soc.*, 2007, **129**, 5932–5938.
- 15 L. Giordano, M. T. Jovin, M. Irie and E. A. Jares-Erijman, *J. Am. Chem. Soc.*, 2002, **124**, 7481–7489.
- 16 S. Maisonneuve, R. Metivier, P. Yu and K. Nakatani, *Beilstein J. Org. Chem.*, 2014, **10**, 1471–1481.
- 17 N. Soh, K. Yoshida, H. Nakajima, K. Nakano, T. Imato, T. Fukamiato and M. Irie, *Chem. Commun.*, 2007, 5206–5208.
- 18 S. Pu, D. Jiang, W. Liu, G. Liu and S. Cui, *J. Mater. Chem.*, 2012, **22**, 3517–3526.
- 19 J. Zhang, W. Tan, X. Meng and H. Tian, *J. Mater. Chem.*, 2009, **19**, 5726–5729.
- 20 M. Berberich, M. Natali, P. Spent, C. Chiorboli, F. Scandola and F. Wurthner, *Chem. Eur. J.*, 2012, **18**, 13651–13664.
- 21 D. E. Williams and N. B. Shustova, *Chem. Eur. J.*, 2015, **21**, 15474–15479.
- 22 K. Liu, Y. Wen, T. Shi, Y. Li, F. Li, Y. L. Zhao, C. Huang and T. Yi, *Chem. Commun.*, 2014, **50**, 9141–9144.
- 23 T. Wu, D. Wilson and N. R. Branda, *Chem. Mater.*, 2014, **26**, 4313–4320.
- 24 S. Xia, G. Liu and S. Pu, *J. Mater. Chem. C*, 2015, **3**, 4023–4029.
- 25 S. A. Diaz, L. Giordano, J. C. Azcarate, T. M. Jovin and E. A. Jares-Erijman, *J. Am. Chem. Soc.*, 2013, **135**, 3208–3217.
- 26 H. B. Cheng, H. Y. Zhang and Y. Liu, *J. Am. Chem. Soc.*, 2013, **135**, 10190–10193.
- 27 Y. Odo, T. Fukaminato and M. Irie, *Chem. Lett.*, 2007, **36**, 240–241.
- 28 J. Wang, Y. Gao, J. Zhang and H. Tian, *J. Mater. Chem. C*, 2017, **5**, 4571–4577.
- 29 Q. Ai, S. Pang and K.H. Ahn, *Chem. Eur. J.*, 2016, **22**, 656–662.
- 30 M. Fredersdorf, R. Gcstl, A. Kolmer, V. Schmidts, P. Monecke, S. Hecht and C. M. Thiele, *Chem. Eur. J.*, 2015, **21**, 14545–14554.
- 31 J. Massaad, J. C. Micheau, C. Coudret, R. Sanchez, G. Guirado and S. Delbaere, *Chem. Eur. J.*, 2012, **18**, 6568–6575.
- 32 Y. Odo, K. Matsuda and M. Irie, *Chem. Eur. J.*, 2006, **12**, 4283–4288.
- 33 S. Yokoyama, T. Hirose and K. Matsuda, *Chem. Eur. J.*, 2015, **21**, 13569–13576.
- 34 Q. Luo, H. Cheng and H. Tian, *Polym. Chem.*, 2011, **2**, 2435–2443.
- 35 S. Z. Pu, Q. Sun, C. B. Fan, R. J. Wang and G. Liu, *J. Mater. Chem. C*, 2016, **4**, 3075–3093.
- 36 J. Luo, Z. Xie, J. W. Y. Lam, L. Cheng, H. Chen, C. Qiu, H. S. Kwok, X. Zhan, Y. Liu, D. Zhu and B. Z. Tang, *Chem. Commun.*, 2001, 1740–1741.
- 37 Z. Yang, Wei Qin, N. L. C. Leung, M. Arseneault, J. W. Y. Lam, G. Liang, H. H. Y. Sung, I. D. Williams and B. Z. Tang, *J. Mater. Chem. C*, 2016, **4**, 99–107.
- 38 R. Singh, A. K. Dwivedi, A. Singh, C. M. Lin, R. Arumugaperumal, K. H. Wei and H. C. Lin, *ACS Appl. Mater. Interfaces*, 2016, **8**, 6751–6762.
- 39 Y. Chen, W. Zhang, Y. Cai, R. T. K. Kwok, Y. Hu, J. W. Y. Lam, X. Gu, Z. He, Z. Zhao, X. Zheng, B. Chen, C. Gui and B. Z. Tang, *Chem. Sci.*, 2017, **8**, 2047–2055.
- 40 R. X. Zhang, P. F. Li, W. J. Zhang, N. Li and N. Zhao, *J. Mater. Chem. C*, 2016, **4**, 10479–10485.
- 41 Y. Ma, Y. Zeng, H. Liang, C. L. Ho, Q. Zhao, W. Huang and W. Y. Wong, *J. Mater. Chem. C*, 2015, **3**, 11850–11856.
- 42 G. Yu, G. Tang and F. Huang, *J. Mater. Chem. C*, 2014, **2**, 6609–6617.
- 43 J. Yang, J. Huang, Q. Li and Z. Li, *J. Mater. Chem. C*, 2016, **4**, 2663–2684.
- 44 N. Zhao, M. Li, J. W. Y. Lam, Y. L. Zhang, Y. S. Zhao, K. S. Wong and B. Z. Tang, *J. Mater. Chem. C*, 2013, **1**, 4640–4646.
- 45 S. Chen, Y. Hong, Y. Liu, J. Liu, C. W. Leung, M. Li, R. T. Kwok, E. Zhao, J. W. Lam, Y. Yu and B. Z. Tang, *J. Am. Chem. Soc.*, 2013, **135**, 4926.
- 46 S. Sasaki, K. Igaw and G.I. Konishi, *J. Mater. Chem. C*, 2015, **3**, 5940–5950.
- 47 Z. Wang, H. Nie, Z. Yu, A. Qin, Z. Zhao and B. Z. Tang, *J. Mater. Chem. C*, 2015, **3**, 9103–9111.
- 48 C. Li, H. Yan, G. F. Zhang, W. L. Gong, T. Chen, R. Hu, M. P. Aldred and M. Q. Zhu, *Chem. Asian J.*, 2014, **9**, 104–109.
- 49 C. Li, W. L. Gong, Z. Hu, M. P. Aldred, G.-F. Zhang, T. Chen, Z. L. Huang and M. Q. Zhu, *RSC Adv.*, 2013, **3**, 8967–8972.
- 50 H. Dong, M. Luo, S. Wang and X. Ma, *Dyes and Pigments*, 2017, **139**, 118–128.

- 51 K. K. Neena and P. Thilagar, *J. Mater. Chem. C*, 2016, **4**, 11465–11473.
- 52 T. Jadhav, B. Dhokale and R. Misra, *J. Mater. Chem. C*, 2015, **3**, 9063–9068.
- 53 H. T. Feng, S. Song, Y. C. Chen, C.H. Shen and Y. S. Zheng, *J. Mater. Chem. C*, 2014, **2**, 2353–2359.
- 54 P. Gopikrishna, D. Das and P. K. Iyer, *J. Mater. Chem. C*, 2015, **3**, 9318–9326.
- 55 R. X. Zhang, P. F. Li, W. J. Zhang, N. Li and N. Zhao, *J. Mater. Chem. C*, 2016, **4**, 10479–10485.
- 56 J. Yang, N. Sun, J. Huang, Q. Li, Q. Peng, X. Tang, Y. Dong, D. Ma and Z. Li, *J. Mater. Chem. C*, 2015, **3**, 2624–2631.
- 57 S. Song, H. F. Zheng, D. M. Li, J. H. Wang, H. T. Feng, Z. H. Zhu, Y. C. Chen and Y. S. Zheng, *Org. Lett.*, 2014, **16**, 2170–2173.
- 58 Z. Wang, J. H. Ye, J. Li, Y. Bai, W. Zhang and W. He, *RSC Adv.*, 2015, **5**, 8912–8917.
- 59 A. Osuka, D. Fujikane, H. Shinmori, S. Kobatake and M. J. Irie, *Org. Chem.*, 2001, **66**, 3913–3923.
- 60 T. B. Norsten and N. R. Branda, *Adv. Mater.*, 2001, **13**, 347–349.
- 61 T. B. Norsten and N. R. Branda, *J. Am. Chem. Soc.*, 2001, **123**, 1784–1785.
- 62 H. C. Kolb, M. G. Finn and K. B. Sharpless, *Angew. Chem. Int. Ed.*, 2001, **40**, 2004.
- 63 A. J. Qin, J. W. Y. Lam and B. Z. Tang, *Chem. Soc. Rev.*, 2010, **39**, 2522.
- 64 G. Franc and A. K. Kakkar, *Chem. Soc. Rev.*, 2010, **39**, 1536.
- 65 P. L. Golas and K. Matyjaszewski, *Chem. Soc. Rev.*, 2010, **39**, 1338.
- 66 A. Qin, J. W. Y. Lam and B. Z. Tang, *Macromolecules* 2010, **43**, 8693–8702.
- 67 L. N. Lucas, J. J. D. De Jong, J. H. Van Esch, R. M. Kellogg and B. L. Feringa, *Eur. J. Org. Chem.*, 2003, 155–166.
- 68 R. Gcstl, B. Kobin, L. Grubert, M. Ptzl and S. Hecht, *Chem. Eur. J.*, 2012, **18**, 14282–14285.
- 69 W. Z. Yuan, Z. Q. Yu, Y. Tang, J. W. Y. Lam, N. Xie, P. Lu, E. Q. Chen and B. Z. Tang, *Macromolecules*, 2011, **44**, 9618–9628.
- 70 J. Bu, K. Watanabe, H. Hayasaka and K. Akagi, *Nat. Commun.*, 2014, **5**, 3799–3806.
- 71 S. Yagai, K. Ishiwatari, X. Lin, T. Karatsu, A. Kitamura and S. Uemura, *Chem. Eur. J.*, 2013, **19**, 6971–6975.
- 72 F. Stellacci, C. Bertarelli, F. Toscano, M. C. Gallazzi, G. Zotti, and G. Zerbi, *Adv. Mater.*, 1999, **11**, 292–295.
- 73 S. Kobatake and M. Irie, *Chem. Lett.* 2003, **32**, 1078–1079.
- 74 K. Higashiguchi, K. Matsuda, Y. Asano, A. Murakami, S. Nakamura and M. Irie, *Eur. J. Org. Chem.*, 2005, **2005**, 91–97.
- 75 K. Morimitsu, S. Kobatake and M. Irie, *Mol. Cryst. Liq. Cryst.*, 2005, **431**, 451–454.
- 76 K. Morimitsu, S. Kobatake, S. Nakamura and M. Irie, *Chem. Lett.*, 2003, **32**, 858–859.
- 77 M. Irie, K. Sakemura, M. Okinaka and K. J. Uchida, *Org. Chem.*, 1995, **60**, 8305–8309.
- 78 K. Shibata, S. Kobatake and M. Irie, *Chem. Lett.*, 2001, **30**, 618–619.
- 79 Q. Luo, H. Cheng and H. Tian, *Polym. Chem.*, 2011, **2**, 2435–2443.
- 80 Z. Li, C. Zhang, Y. Ren, J. Yin and S. H. Liu, *Org. Lett.*, 2011, **22**, 6022–6025.
- 81 F. Hu, M. Hu, W. Liu, J. Yin, G. A. Yu and S. H. Liu, *Tetrahedron Letters*, 2015, **56**, 452–457.
- 82 R. Bauernschmitt and R. Ahlrichs, *Chem. Phys. Lett.*, 1996, **256**, 454–64.
- 83 F. Hu, M. Hu, W. Liu, J. Yin, G. A. Yu and S. H. Liu, *Tetrahedron Lett.*, 2015, **56**, 452–457.

Graphical abstract

